Dyes and Pigments 95 (2012) 102–111

Contents lists available at SciVerse ScienceDirect

Dyes and Pigments

journal homepage: www.elsevier.com/locate/dyepig

Modeling the adsorption of textile dye on organoclay using an artificial neural network

Seniha Elemen [a], Emriye Perrin Akçakoca Kumbasar [a,*], Saadet Yapar [b]

[a] Ege University, Engineering Faculty Textile Engineering Department, 35100 Bornova, Izmir, Turkey
[b] Ege University, Engineering Faculty Chemical Engineering Department, 35100 Bornova, Izmir, Turkey

ARTICLE INFO

Article history:
Received 28 November 2011
Received in revised form
17 February 2012
Accepted 1 March 2012
Available online 21 March 2012

Keywords:
Reactive dye
Textile wastewater
Decolorization
Adsorption
Organoclay
Artificial neural network

ABSTRACT

Decolorization of Reactive Red 141 by an organoclay was investigated. The organoclay was synthesized in laboratory conditions by using a cationic surfactant (hexadecyltrimethylammoniumbromide) in an amount equivalent to 100% of the cation exchange capacity of bentonite. The surface modification of bentonite with the surfactant was examined using X-ray diffraction and the Fourier transform infrared spectroscopic technique. Adsorption isotherms and equilibrium adsorption capacities were determined by the fitting of the experimental data to three well-known isotherm models: Langmuir, Freundlich and Sips (Langmuir–Freundlich). Results indicated that the decolorization was dependent on contact time, initial dye concentration, adsorbent dosage and temperature. An artificial neural network model was developed to predict the decolorization of the Reactive Red 141 solution. It was concluded that artificial neural network provided reasonable predictive performance. Simulations based on the developed artificial neural network model can estimate the behavior of the decolorization process under different conditions.

1. Introduction

The textile industry has used synthetic dyes extensively and the dyes most commonly used in textile dyeing processes are reactive dyes [1–3]. Although these dyes have brilliant color and high fastness, they are among the most problematic dyes in washing compared to other forms of dyes. Reactive dyes are water soluble, but a considerable amount of these dyes are hydrolyzed during dyeing. Thus, nearly 10–50% of the initial dye cannot react with the fiber being dyed and are discharged with the wastewater [3,4].

The removal of color from textile effluents is a major problem because the dyes cause remarkable environmental pollution and have toxic and carcinogenic effects on living beings. In addition, the presence of very low concentrations of colored effluents is highly visible and potentially inhibiting to photosynthesis. As a result, textile wastewater treatment has become an important issue [2–5].

Since conventional physicochemical coagulation/flocculation methods have failed at treating reactive dyes, adsorption has been turned to as one of the most effective and low-cost wastewater treatment methods [2–6]. There are many kinds of adsorbents for removing textile dyes from wastewater. Activated carbon is one of the most available adsorbents. However, the relatively high production and regeneration cost of activated carbon and approximately 10–25% loss during regeneration by chemical or thermal treatment makes this adsorbent economically less applicable. Therefore much research concerning adsorbents made from natural sources such as clays, zeolites, sawdust and/or other low-cost and available solid materials to remove dyes from wastewater has been undertaken [1,3,6,7]. Among these adsorbents, clay minerals (especially organoclays) are widely used as adsorbents in studies of textile wastewater treatment [8–19].

Clay minerals are suitable for adsorption process due to their large specific surface area and nanometer scale size [12]. Also, clays can be modified by the intercalation of organic cations into their interlayer surface. After the modification, the clays become organophilic and the negative charges of the clay surfaces are neutralized. Thus organoclays are attractive for use as selective sorbents due to the organic layer [20,21].

The behavior of adsorption of the anionic dyes onto polydiallydimethylammonium–modified bentonite (PDADMA–bentonite) was studied in single, binary and ternary dye systems by Shen et al. [13]. They found that PDADMA–bentonite can be used as a low-cost adsorbent to remove anionic dyes, namely Acid

* Corresponding author. Ege Universitesi, Muh. Fak., Tekstil Muh. Böl., 35100 Bornova, Izmir, Turkey. Tel./fax: +90 232 339 9222.
E-mail address: perrin.akcakoca@ege.edu.tr (E.P. Akçakoca Kumbasar).

0143-7208/$ – see front matter © 2012 Elsevier Ltd. All rights reserved.
doi:10.1016/j.dyepig.2012.03.001

Scarlet GR (AS-GR), Acid Turquoise Blue 2G (ATB-2G) and Indigo Carmine (IC). Zohra et al. [14] reported that cetyltrimethylammonium bromide–bentonite (CTAB–bentonite) can be used to remove colored textile dyes from wastewater. They researched the adsorption of the direct dye (Benzopurpurin 4B) by CTAB–bentonite and they found that CTAB–bentonite is an effective adsorbent for removing Benzopurpurin 4B from aqueous solutions. Yang et al. [15] determined that nanoclay (modified montmorillonite) has a high sorption capacity for the textile dyes. They studied the effects of aromatic and aliphatic groups (Cloisites 10A and 15A, respectively), the effects of the hydroxyl group (Cloisite 30B), and the charge effects (positive for Cloisites 10A 15A and 30B and negative for Na^+ clays in water) on sorption of textile dyes (C.I. Acid Red 266, Direct Red 80, Reactive Blue 19, Basic Red 2 and Disperse Red 65). In this study, it was found that Van der Waals forces and hydrophobic interactions were the two major forces for dye sorption onto clay, and that ionic attraction also played an important role. Juang et al. [16] reported that hexadecyltrimethylammonium (HDTMA) chloride modified montmorillonite might be a good adsorbent for the removal of acid dye (Amido Naphthol Red G, AR1) from wastewater. The ability of bentonite to remove Malachite Green from aqueous solutions has been investigated by Thir et al. [17]. It was observed that removal of >90% of dye was achieved by using 0.05 g of bentonite. Bouberka et al. [18] used different clays (clay exchanged with sodium {BNa^+} and hydroxyaluminic polycation pillared clays in the presence or absence of non-ionic surfactants) for the removal of the pollutant Supranol Yellow 4GL (S.Y.4GL). Al-pillared and Al-modified clays exhibit a high adsorption capacity for the anionic dye Supranol Yellow 4GL with respect to the starting montmorillonite BNa^+. Previous studies show that the modified clay has potential in the removal of some textile dye through adsorption.

However, there are few studies concerning the ability of organoclays to adsorb reactive dyes [19,22,23], although reactive dyes are a very important class of textile dyes because of their low fixation level and removal rate in treatment stations [24,25]. Based on a review of the available literature, the authors believe that the present study examines for the first time both the adsorption behavior of HDTMA–bentonite in relation to reactive dye, and the modeling of adsorption studies by artificial neural networks.

The artificial neural network (ANN) method is a modeling method that can introduce mathematical functions for both linear and non-linear systems. It has been widely used in various research areas where the experimental information is available. It can also be used for water treatment model development [26].

Daneshvar et al. [27] have studied the removal of color from solutions containing C.I. Basic Yellow 28 using the electrocoagulation method. They have also developed an ANN model to predict the performance of decolorization efficiency by the electrocoagulation process based on experimental data obtained in a laboratory batch reactor. The input parameters such as current density, initial pH of the solution, time of electrolysis, initial dye concentration, distance between the electrodes, retention time and solution conductivity were studied to predict the color removal. They found that the ANN model can describe the percentage color removal under different conditions.

Photocatalytic removal of C.I. Basic Red 46 using TiO_2 nanoparticles irradiated by a 30 W UV-C lamp in a batch reactor has been investigated by Khataee [28]. In this study initial dye concentration, UV light intensity, time and initial pH were studied and the experimental data were then developed using ANN. It was found that the ANN method provided reasonable predictive performance ($R^2 = 0.96$).

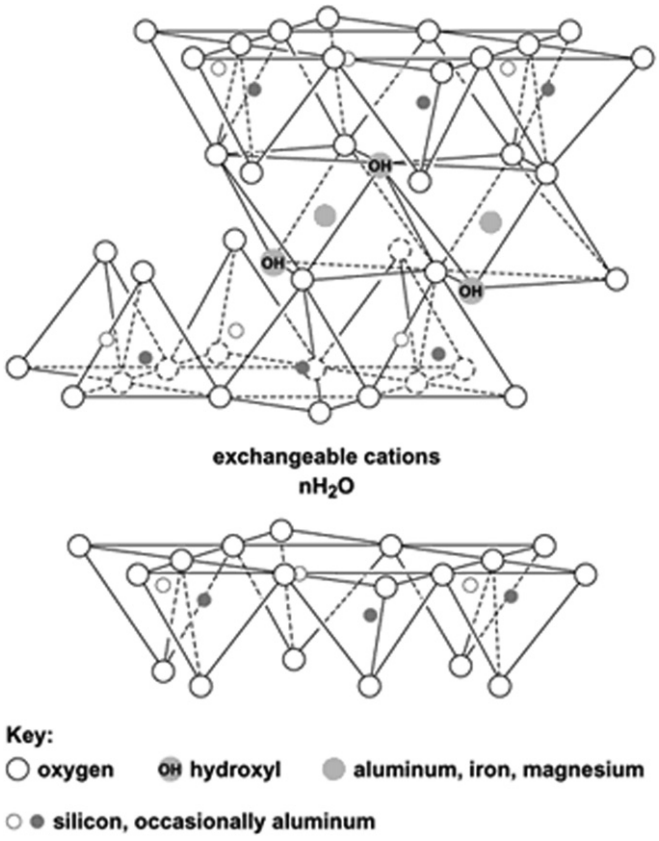

Fig. 1. Structure of montmorillonite [32].

Salari et al. [29] used the peroxi-coagulation process to assess the decolorization of C.I. Basic Yellow 2 (BY2) in aqueous solutions. They studied the effect of operational parameters such as applied current, initial pH and initial dye concentration in an attempt to reach higher decolorization efficiency. They successfully used artificial neural network modeling to investigate the cause–effect relationship in the peroxi-coagulation process ($R^2 = 0.97$).

Biological decolorization of the triphenylmethane dye Malachite Green (MG) by three microalgae (the *Chlorella*, *Cosmarium* and *Euglena* species) has been investigated by Khataee et al. [30]. They developed an artificial neural network (ANN) model to predict the biological decolorization of MG solutions. They reported that the developed ANN model could describe the behavior of the complex interaction process within the range of experimental conditions adopted ($R^2 = 0.98$).

Balci et al. [31], have studied the adsorption process of textile dyes (Basic Blue 41 − BB41 and Reactive Black 5 −RB5) in glass columns using tree barks (*Eucalyptus camaldulensis*). They developed an artificial neural network (ANN) based model for determining the dye adsorption capability of bed systems. They observed that the ANN-predicted results were very close to the experimental values. They also found that mean square errors in BB41 and RB5 test data were 0.00620594 and 0.00119229 respectively, which are within ±1% error range.

The objective of the present study was to analyze the functions of initial dye concentration, adsorbent dosage, temperature, and contact time in a batch system on the removal of the textile dye Reactive Red 141 (RR 141) from aqueous solutions using an organoclay. A three-layer ANN model using a backpropagation algorithm was used to predict the efficiency of organoclay as an adsorbent material in RR 141 removal.

2. Experimental

2.1. Materials

The bentonite which consists of montmorillonite was obtained from the Tokat Reşadiye region of Turkey. Fig. 1 shows an example of the structure of montmorillonite [32]. First the impurities such as iron oxide and silica were removed by a sedimentation method. Then the samples were dried in an oven at 60 °C and pulverized to pass through a 530 μm sieve. The cation exchange capacity (CEC) of bentonite is 0.91 mequiv/g, according to calculations by Yılmaz and Yapar [21].

The organic cation as quaternary ammonium is hexadecyltrimethylammonium bromide [$CH_3(CH_2)_{15}N(CH_3)_3Br$], (HDTMAB, Merck) with 99% purity.

The dye, C.I. Reactive Red 141, was obtained from DyStar. The chemical constitution of the dye is illustrated in Fig. 2 [33].

2.2. Preparation of HDTMA-exchanged bentonite (organo-bentonite)

Clay–water dispersion and HDTMAB solution in amounts equal to 100% of CEC were prepared according to the literature [20]. Then these two solutions were mixed together and the mixture was microwaved for 5 min at 360 W in a microwave oven (Beko). After that the modified clay was washed with distilled water and filtered to remove the surfactants which do not react with clay. This step was carried out until the amount of HDTMAB observed in the filtrate was no longer significant. The amount of surfactant in the filtrate was determined by the methyl orange method [34]. After the washing step, the sample was dried by a Labconco FreeZone 2.5 model freeze-dryer at a temperature of −45 °C and a pressure of 0.06 mbar for 8 h.

2.3. Material characterization

The X-ray diffraction (XRD) measurements were collected using a Philips X'Pert Pro diffractometer between 2° and 40° (2θ).

The nature of surface species was determined by Fourier transform infrared spectroscopy (FTIR) using a Perkin–Elmer spectrophotometer.

2.4. Adsorption experiments

The functions of initial dye concentration (20–200 mg L^{-1}), adsorbent dosage (0.05–0.1 g L^{-1}), temperature (30–40 °C) and contact time (0–1440 min) on the dye adsorption were studied. These studies were carried out in 100 mL conical flasks containing 50 mL of the adsorption solution with desired dye concentration and adsorbent value. These flasks were stirred on the orbital shaker (Nüve, ST 402) at different temperatures for various time periods. During adsorption studies, the supernatants of the solutions were separated by centrifugation from the organoclay by using a centrifuge (Nüve, NF 400). Before absorbance measurement, the clay was filtered from the dye liquor to assure that small clay particles did not interfere with the absorbance measurement. The residual dye concentration in the supernatant liquid was analyzed using a UV–vis spectrophotometer (Perkin–Elmer Lambda 25) at 519 nm. Each data point was the mean of three independent adsorption studies.

Table 1
The parameter R_L indicated the shape of isotherm [35].

Value of R_L	Type of isotherm
$R_L > 1$	Unfavorable
$R_L = 1$	Linear
$0 < R_L < 1$	Favorable
$R_L = 0$	Irreversible

The data were used to calculate the adsorption capacity (mg/g), q_e, of the adsorbent. Finally, the adsorption capacity was plotted against the equilibrium concentration (mg/l), C_e. The dye concentration on the adsorbent surface at equilibrium was calculated by [14]:

$$q_e = \frac{(C_0 - C_e)V}{m} \quad (1)$$

where C_0, initial dye concentration in liquid phase (mg/l); V, total volume of dye solution used (L); m, mass of adsorbent used (g).

Kinetic studies were also carried out by shaking the dispersions, which contained Reactive Red 141 dye at 100 mg l^{-1} initial concentration, over a time interval of 0–24 h for all adsorbent dosages and temperatures.

2.5. Adsorption isotherms

The Langmuir equation is given in Eq. (2) [35]:

$$q_e = \frac{q_{max}K_L C_e}{1 + K_L C_e} \quad (2)$$

where q_{max} is the maximum adsorption capacity corresponding to complete monolayer coverage on the surface (mg/g) and K_L is the Langmuir constant (L/mg). Eq. (2) can be written in a linear form [35]:

$$\frac{C_e}{q_e} = \frac{1}{q_{max}K_L} + \frac{C_e}{q_{max}} \quad (3)$$

The constants can be evaluated from the intercepts and the slopes of the linear plots of C_e/q_e versus C_e.

The dimensionless separation factor, R_L, can be defined as an essential characteristic of the Langmuir equation. It can be written as [35]:

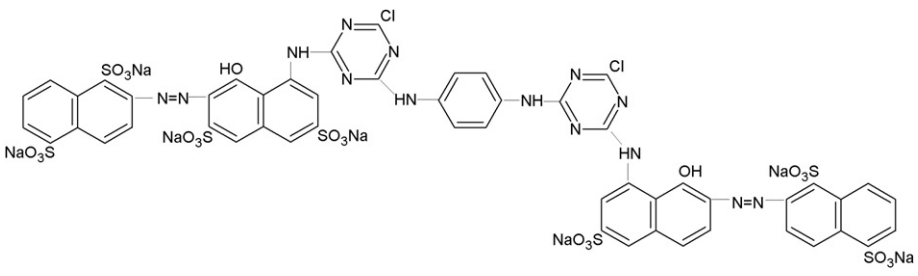

Fig. 2. Chemical structure of C.I. Reactive Red 141 [33].

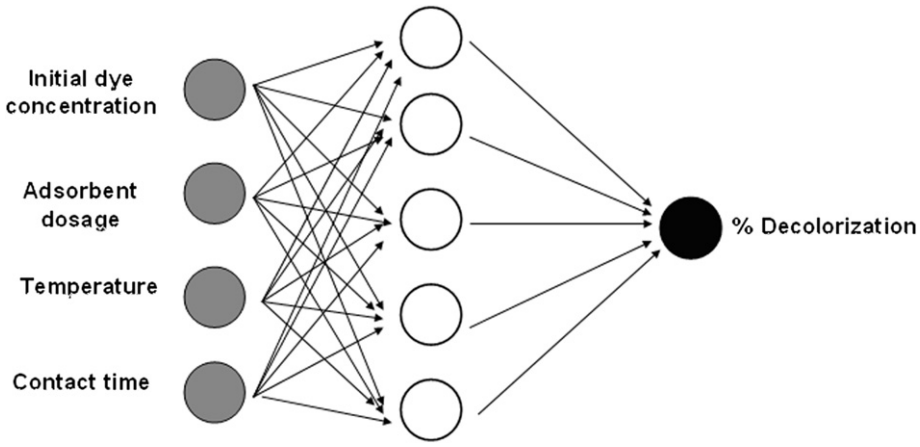

Fig. 3. Structure of the ANN.

$$R_L = \frac{1}{1 + K_L C_H} \tag{4}$$

where C_H is the highest initial solute concentration and K_L is the Langmuir adsorption constant (L/mg). Table 1 shows the parameter R_L indicated the shape of isotherm.

The Freundlich equation describes heterogeneous systems. It can be characterized by the heterogeneity factor $1/n$. The equation can be defined as [35]:

$$q_e = K_F C_e^{1/n} \tag{5}$$

where K_F is the Freundlich constant (mg/g)(L/mg)$^{1/n}$ and $1/n$ is the heterogeneity factor. A linear form of the Freundlich model can be written by taking logarithms of Eq. (5):

$$\ln q_e = \ln K_F + \frac{1}{n} \ln C_e \tag{6}$$

The constant K_F and exponent $1/n$ can be obtained from the intercepts and the slopes of the linear plots of $\ln q_e$ versus $\ln C_e$ [35].

The Sips isotherm is a simple generalization of the Langmuir and Freundlich isotherms. The equation is defined as [36]:

$$q_e = \frac{q_{m_S} K_S C_e^{m_S}}{1 + K_S C_e^{m_S}} \tag{7}$$

where q_{m_S} is the Sips maximum adsorption capacity (mg/g), K_S is the Sips equilibrium constant (L/mg)^m, and m_S is the Sips model exponent.

2.6. Adsorption kinetics

There are several kinetic models that characterize the adsorption process. Two of the most frequently used models are the pseudo-first-order kinetic model and the pseudo-second-order kinetic model.

The pseudo-first-order kinetic model is given by Eq. (8):

$$\frac{dq_t}{dt} = k_1 (q_e - q_t) \tag{8}$$

By taking $q_t = 0$ at $t = 0$ and $q_t = q_t$ at time t, the integrated form of Eq. (8) becomes:

$$\ln\left(\frac{q_e}{q_e - q_t}\right) = k_1 t \tag{9}$$

where q_t is the amount of adsorbed dye at time t, and k_1 is the rate constant of first-order sorption. The parameters of the equation can be obtained from the linear plot of $\ln(q_e - q_t)$ versus t.

Another model for the analysis of sorption kinetics is the pseudo-second-order kinetic model. This model is expressed as:

$$\frac{dq_t}{dt} = k_2 (q_e - q_t)^2 \tag{10}$$

where k_2 is the pseudo-second-order rate constant of sorption. As in Eq. (8), by taking $q_t = 0$ at $t = 0$ and $q_t = q_t$ at time t, the integrated form of Eq. (10) becomes

$$\frac{t}{q_t} = \frac{1}{k_2 q_e^2} + \frac{t}{q_e} \tag{11}$$

The plot of t/q versus t gives a straight line with a slope of $1/k_2 q_e^2$ and an intercept of $1/q_e$ [37].

2.7. Artificial neural network (ANN)

In this study, the Neural Network Toolbox of MATLAB 7.10 (R2010a) mathematical software was used to predict adsorption efficiency. Input variables to the feed-forward neural network were as follows: initial dye concentration (20–200 mg L^{-1}), adsorbent dosage (0.05–0.1 g L^{-1}), temperature (30–40 °C) and contact time (0–1440 min). The decolorization efficiency of the dye was chosen as the output variable (Fig. 3). 100 experimental data points were used to feed the ANN structure. The samples were allocated to training and test sets that contained 85 and 15 samples, respectively. A three-layer ANN with *log-sigmoid* transfer functions with a backpropagation algorithm was designed for this study.

The sigmoidal transfer function, which was used in this work, is given by Eq. (12):

$$f(S) = \frac{1}{1 + e^{-S}} \tag{12}$$

Since the transfer function used in the hidden layer was sigmoid, all samples were scaled in 0–1 ranges. A linear transfer function (*purelin*) was used at the output layer. The training function was "train scaled conjugate gradient backpropagation" (*trainscg*). The mean square error (MSE) was used as the error function (Eq. (13)).

$$\mathrm{MSE} = \frac{1}{n} \sum_{i-1}^{n} \left(y_{i,\mathrm{nn}} - y_{i,\mathrm{exp}}\right)^2 \tag{13}$$

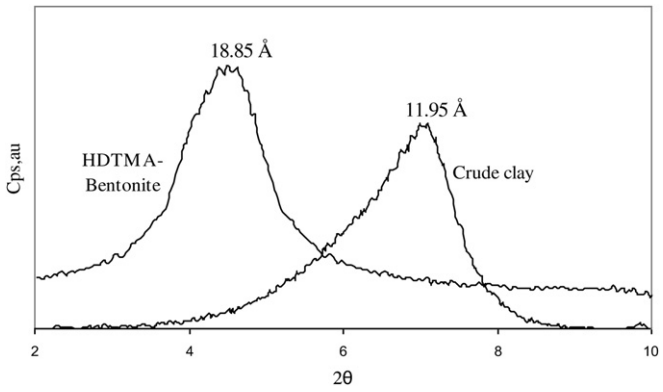

Fig. 4. X-ray diffraction patterns of crude clay and HDTMA–bentonite.

where n is the number of data points, $y_{i,nn}$ is the network prediction, $y_{i,exp}$ is the experimental response and i is an index of the data [38].

The most suitable network model, which produces the minimum value of mean square error (MSE), was found using a trial and error method. The maximum number of epochs and the number of neurons in the hidden layer were selected as 500 and 5, respectively.

3. Results and discussions

3.1. XRD analysis

The basal spacing (d_{001}) of crude bentonite and organo-bentonite are 11.95 and 18.85 Å, respectively (Fig. 4). This result indicates the existence of quaternary ammonium cations in the interlayer of the clay.

3.2. FTIR analysis

FTIR spectra of crude bentonite and organo-bentonite are depicted in Fig. 5. A pair of strong bands at 2850 and 2922 cm^{-1} was observed in organo-bentonite. They can be assigned to the symmetric and asymmetric stretching vibrations of the methyl and methylene groups and their bending vibrations are between 1468 and 1475 cm^{-1}, supporting the intercalation of surfactant molecules between the silica layers, but these stretching and bending bands are not observed in crude bentonite. This may be acceptable evidence for the surface modification occurring in bentonite.

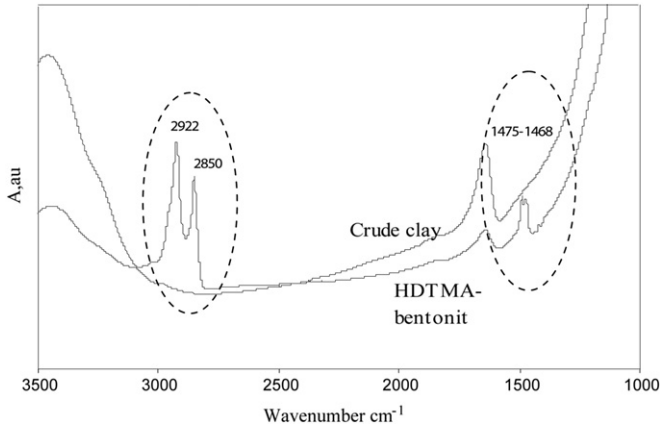

Fig. 5. FTIR spectra of crude clay and HDTMA–bentonite.

Table 2
The adsorption results obtained from experiments with crude clay.

C_i	A_i	A_f	C_f
0.02	0.1971	0.1891	0.01549
0.04	0.4168	0.4153	0.04233
0.06	0.6945	0.6811	0.06870
0.08	0.8777	0.8651	0.08184
0.1	1.1161	1.0571	0.10358
0.12	1.2831	1.2621	0.12368

C_i: initial dye concentration (g/l).
A_i: absorbance value of initial dye solution.
A_f: absorbance value of final dye solution.
C_f: final dye concentration (after adsorption) (g/l).

Table 3
The Langmuir isotherm parameters for HDTMA–bentonite.

Adsorbent dosage (g)	Temperature (°C)	q_{max} (mg/g)	K_L (L/mg)	R_L	R^2	ΔQ ($\times 10^2$)
0.05	30	153.47	0.52	0.009	0.999	1.72
	40	151.75	0.40	0.012	0.999	1.83
0.1	30	104.48	1.63	0.003	0.987	0.75
	40	104.63	1.23	0.004	0.990	0.21

3.3. Adsorption isotherms

The adsorption studies were conducted primarily with crude clay. Table 2 shows the results of dye adsorption by crude clay.

As given in Table 2, the absorbance values of the initial dye solution and the absorbance values of the final dye solution after the adsorption process are very close to each other. Also, the initial dye concentration and the final dye concentration were found to be approximately equal to each other. It can be seen from these results that Reactive Red 141 cannot be adsorbed by the crude clay. The crude clay has an anionic and hydrophilic nature and reactive dyes are one of the anionic dye classes. Due to the resultant lack of interaction between reactive dyes and crude clay, this clay is ineffective for dye adsorption.

The structure of Si–O groups and hydration of Na^+ ions in the clay establishes a hydrophilic structure on the mineral surface. Crude clay is a relatively ineffective adsorbent for organic molecules. However, the anionic surface properties of the clay can

Table 4
The Freundlich isotherm parameters for HDTMA–bentonite.

Adsorbent dosage (g)	Temperature (°C)	$1/n$	K_F $(mg/g)(L/mg)^{1/n}$	R^2	ΔQ ($\times 10^2$)
0.05	30	0.22	67.88	0.819	6.33
	40	0.23	63.03	0.823	6.24
0.1	30	0.38	57.70	0.935	1.29
	40	0.37	51.88	0.933	1.16

Table 5
The Sips isotherm parameters for HDTMA–bentonite.

Adsorbent dosage (g)	Temperature (°C)	q_{m_s} (mg/g)	K_S $(L/mg)^m$	m_S	R^2	ΔQ ($\times 10^2$)
0.05	30	153.46	0.52	1	0.976	1.71
	40	151.75	0.40	1	0.985	1.81
0.1	30	152.52	0.52	0.64	0.981	0.59
	40	131.33	0.64	0.73	0.980	0.60

be changed using positively charged organic compounds such as alkyl ammonium ions. The modified surface of the clay (HDTMA–bentonite for this study) becomes hydrophobic and organic molecules can therefore interact strongly with it. Textile dyes are large organic molecules and they can be adsorped by modified clay due to the hydrophobic interaction between the dye molecules and the modified clay.

The present study examined HDTMA–bentonite in order to obtain adsorption isotherms. The different experimental isotherms were modeled according to three equations — the Langmuir, Freundlich and Sips isotherm models — using Excel software and the Excel Solver tool.

r^2 values of the equations were analyzed to determine the suitability of the isotherms. Normalized deviation values (ΔQ) were also calculated for each isotherm. ΔQ values were calculated from:

$$\Delta Q = \frac{1}{N}\sum[(Q_h - Q_d)/Q_d] \quad (14)$$

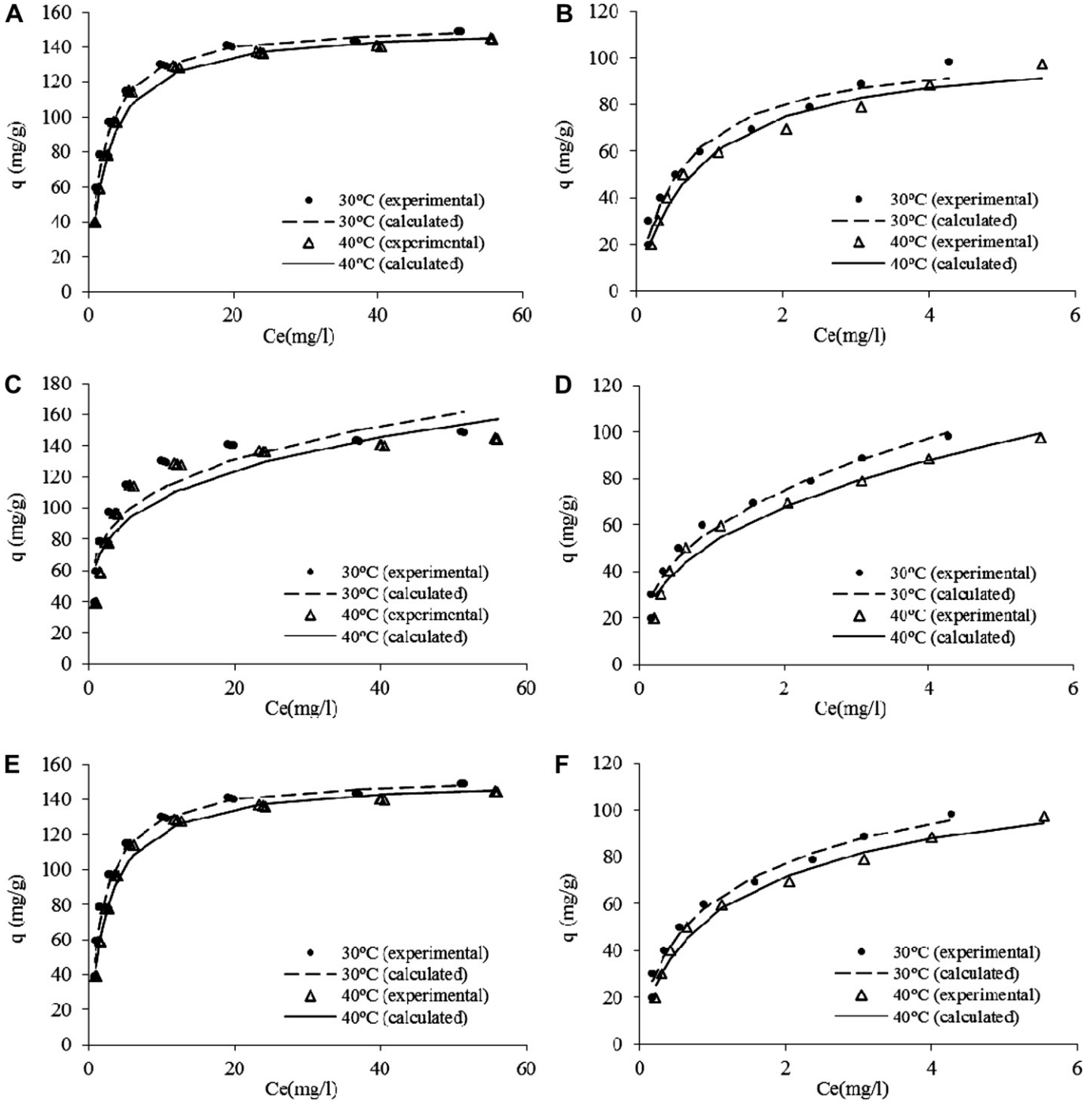

Fig. 6. Adsorption isotherms of dye adsorption on HDTMA–bentonite. (A) Langmuir isotherm with 0.05 g adsorbent; (B) Langmuir isotherm with 0.1 g of adsorbent; (C) Freundlich isotherm with 0.05 g of adsorbent; (D) Freundlich isotherm with 0.1 g of adsorbent; (E) Sips isotherm with 0.05 g of adsorbent; (F) Sips isotherm with 0.1 g of adsorbent.

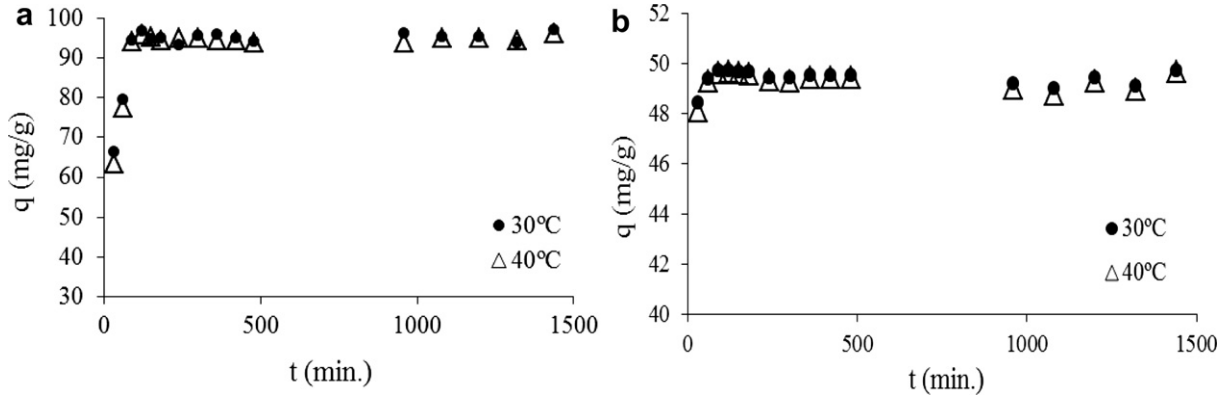

Fig. 7. Amounts of the dye adsorbed versus contact time for HDTMA–bentonite with (a) 0.05 g of adsorbent, and (b) 0.1 g of adsorbent.

Tables 3–5 show the correlation coefficients and the normalized deviation values for the Langmuir, Freundlich and Sips sorption isotherm constants, respectively.

When the r^2 and ΔQ values are compared, the equilibrium data of the reactive dye onto the organo-bentonite follow the Langmuir isotherm. The correlation coefficient values of Langmuir isotherms for the organo-bentonite indicate that there is a strong positive relationship for the data. In addition, the m_s values of the Sips model for the adsorbent dosage of 0.05 g were found to be 1, thus the model turned into the Langmuir model. This shows again that the adsorption behavior of reactive dye on organo-bentonite fits the Langmuir equation.

In addition, the calculated R_L values which are the one of the Langmuir isotherm characteristics were found to be between 0 and 1 for the all adsorbent dosages and temperatures. These results indicate that adsorption is favorable according to Table 1.

Adsorption isotherms with experimental and calculated data obtained from dye adsorption are shown in Fig. 6.

The adsorption isotherms of the dye point to increasing adsorbate–adsorbent interactions with increasing initial dye concentrations (Fig. 6). Thus the amounts of adsorbed dye increase with the increase in initial dye concentrations until the equilibrium point is reached. Also there is no significant difference between the adsorption isotherms at two different temperatures, 30 °C and 40 °C.

3.4. Adsorption kinetics

The change in adsorbed amounts with time is given in Fig. 7a and b. The time to reach the plateau is about the same (approximately 90–120 min) for different temperature and adsorbent dosage.

The first-order kinetic equation (Eq. (9)) and pseudo-second-order equation (Eq. (11)) were applied to the data. The parameters of the kinetic models and correlation coefficients are given in Tables 6 and 7.

The values of the correlation coefficient imply that the adsorption of the dye on HDTMA–bentonite is described by a pseudo-second-order equation.

3.5. Effects of adsorbent dosage

Dye solutions with different initial concentrations in the range of 20–200 mg l^{-1} were treated by HDTMA–bentonite for 24 h at different temperatures. The experimental and ANN predicted values of color removal percent were plotted against related initial dye concentrations (Fig. 8).

When the graphs in Fig. 8 are compared with each other, it can be seen that color removal increases with increasing amounts of adsorbent regardless of initial dye concentration. The percentage of dye removed was approximately constant for 0.1 g of adsorbent over the concentration range studied.

However, the percentage of dye removed by 0.05 g of adsorbent decreased when the initial dye concentration increased. Up to the concentration of 80 mg l^{-1}, the adsorption capacity of HDTMA–bentonite was not exhausted and the rate of color removal was relatively constant. Beyond this concentration, the adsorption capacity of HDTMA–bentonite became exhausted.

3.6. ANN studies

An artificial neural network was used for modeling the adsorption studies. Experimental data obtained under different operating conditions were used to train and test the neural network model.

In Fig. 8, it can be seen that the experimental results and the predicted results by ANN are compatible with each other.

The different algorithms and transfer functions that were tested are given in Table 8. The table shows that the "scaled conjugate gradient backpropagation" algorithm gives the most satisfactory results. Among the transfer functions used, "logsig" is the most suitable for adsorption efficiency calculation. The

Table 6
Parameters of the pseudo-first-order equation.

Adsorbent dosage (g)	t (°C)	q_e	k_1 (s^{-1})	R^2
0.05	30	108.69	20.52	0.294
	40	109.89	22.80	0.333
0.1	30	54.35	6.34	0.039
	40	54.34	6.45	0.040

Table 7
Parameters of the pseudo-second-order equation.

Adsorbent dosage (g)	t (°C)	q_e (mg g^{-1})	k_2 (dm^3 mol^{-1} s^{-1})	R^2
0.05	30	96.15	0.0024	0.999
	40	95.23	0.0023	0.999
0.1	30	49.26	0.0491	0.999
	40	49.26	0.0424	0.999

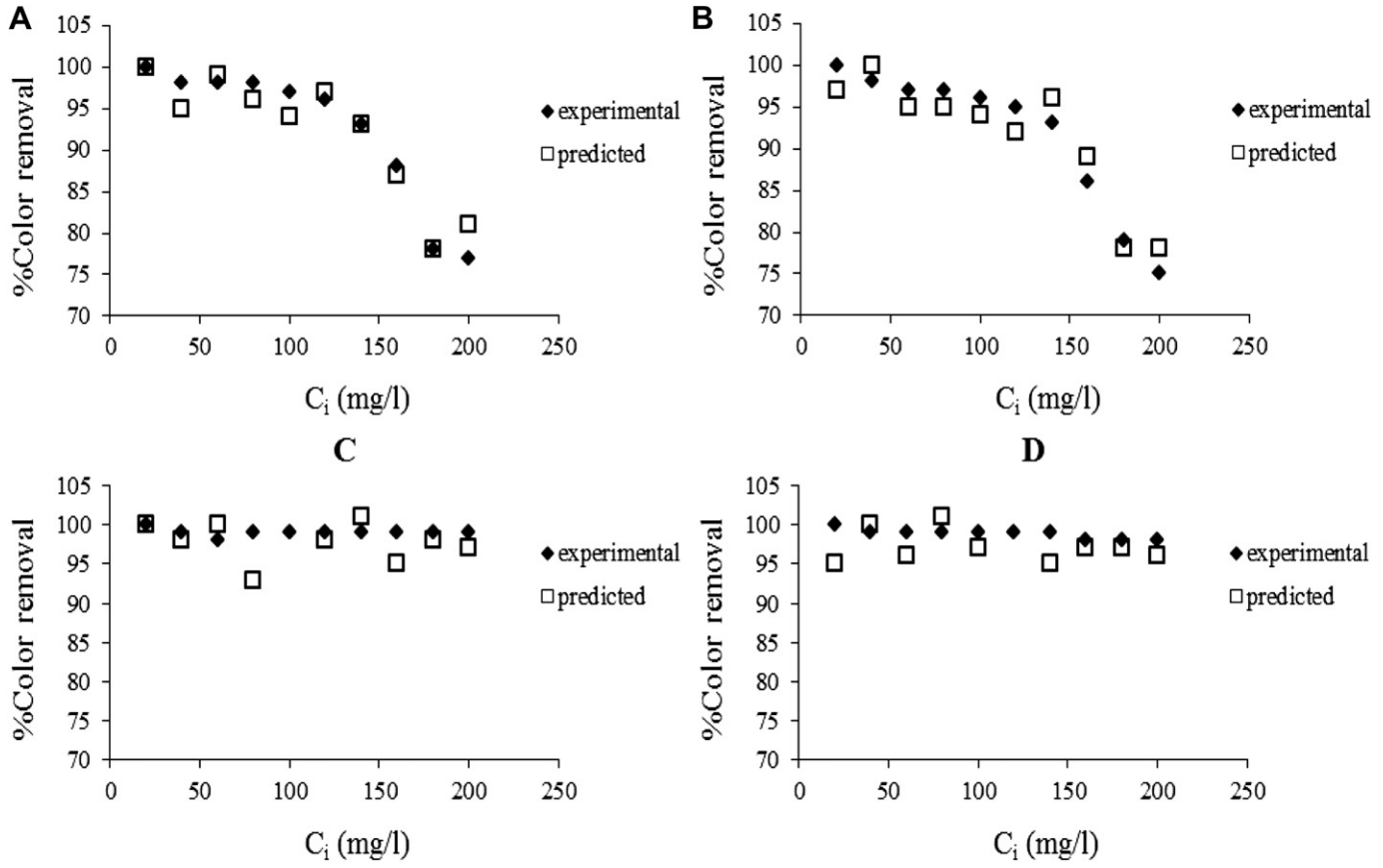

Fig. 8. Color removal percent with experimental results and predicted results by ANN. The adsorption conditions: (A) 30 °C, 0.05 g of adsorbent; (B) 40 °C, 0.05 g of adsorbent; (C) 30 °C, 0.1 g of adsorbent (D) 40 °C, 0.1 g of adsorbent. (Contact time is 24 h for all adsorption processes).

hyperbolic tangent sigmoid transfer function, "tansig", is quite satisfactory for some cases. The results from using the most suitable combination of the "scaled conjugate gradient backpropagation" algorithm and the "logsig" transfer function are given in Fig. 9.

Fig. 9 shows a comparison between experimental and predicted values of the output variable by using the neural network model. The plot in this figure has a correlation coefficient of 0.978. The MSE value was found to be 0.027364. These results confirmed that the neural network model reproduces the decolorization

Table 8
Summary of trial and error method used for adsorption efficiency ANN model development.

Algorithm	Function	Transfer function for hidden layer	Transfer function for output layer	Correlation coefficient (R^2)	Mean square error (MSE)
Scaled conjugate gradient backpropagation	trainscg	logsig	purelin	0.97	0.027364
		tansig		0.87	0.025364
		poslin		0.83	0.11193
Levenberg–Marquardt backpropagation	trainlm	logsig	purelin	0.91	0.039921
		tansig		0.92	0.11825
		poslin		0.82	0.11357
Gradient descent with momentum backpropagation	traingdm	logsig	purelin	0.58	0.15655
		tansig		0.51	0.18299
		poslin		0.67	0.17413
Conjugate gradient backpropagation with Powell–Beale restarts	traincgp	logsig	purelin	0.91	0.082202
		tansig		0.92	0.11452
		poslin		0.84	0.096518
Resilient backpropagation	trainrp	logsig	purelin	0.88	0.12522
		tansig		0.90	0.12868
		poslin		0.84	0.16308

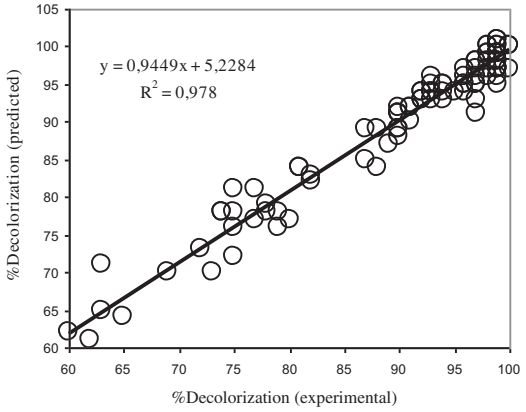

Fig. 9. ANN-predicted decolorization percentages versus experimental ones.

values for this system, within the experimental ranges adopted in the fitting model.

4. Conclusion

The potential for the use of organoclay (HDTMA–bentonite) for the removal of reactive dye was investigated in this study. Adsorption of the dye was studied by batch technique and it was observed that by using HDTMA–bentonite approximately >80% of the dye was removed. The study suggested strongly that organoclay might be a suitable adsorbent for the removal of reactive dye from wastewater.

The surface modification of bentonite was tested by using the XRD and FTIR techniques. The straight line obtained for the Langmuir model fits well with the experimental equilibrium data. The R_L values showed that organoclay was favorable for the adsorption of RR 141 dye (Table 3).

The adsorption performance of organo-bentonite in the treatment of RR 141 solutions was successfully predicted by applying a three-layered neural network with 5 neurons in the hidden layer, and using a backpropagation algorithm. An analysis of the relationship between the predicted results of the designed ANN model and the experimental data was also conducted. As a result of using the ANN model, the values of the determination coefficient (R^2) and the mean square error were found to be 0.978 and 0.027364, respectively.

Acknowledgment

The authors would like to gratefully acknowledge the financial support for this research received through Project no. 109M752 of The Scientific and Technical Research Council of Turkey (TUBITAK); through Project no. DPT-2007K 120780 of the T.R. Prime Ministry State Planning Organization; and through Project no. 10MUH034 of Ege University's scientific research projects. We also thank Mr. Aybars Uğur for assistance in using ANN for the modeling of decolorization processes.

References

[1] Özcan A, Öncü EM, Özcan AS. Kinetics, isotherm and thermodynamic studies of adsorption of Acid Blue 193 from aqueous solutions onto natural sepiolite. Colloids Surf A Physicochem Eng Asp 2006;277:90–7.
[2] Lee JW, Choi SP, Thiruvenkatachari R, Shim WG, Moon H. Evaluation of the performance of adsorption and coagulation processes for the maximum removal of reactive dyes. Dyes Pigments 2006;69:196–203.
[3] Özdemir O, Armagan B, Turan M, Çelik MS. Comparison of the adsorption characteristics of azo-reactive dyes on mezoporous minerals. Dyes Pigments 2004;62:49–60.
[4] Al-Degs Y, Khraisheh MAM, Allen SJ, Ahmad MN. Effect of carbon surface chemistry on the removal of reactive dyes from textile effluent. Water Res 2000;34:927–35.
[5] Hameed BH, Ahmad AL, Latiff KNA. Adsorption of basic dye (methylene blue) onto activated carbon prepared from rattan sawdust. Dyes Pigments 2007;75:143–9.
[6] Arami M, Limaee NY, Mahmoodi NM, Tabrizi NS. Equilibrium and kinetics studies for the adsorption of direct and acid dyes from aqueous solution by soy meal hull. J Hazard Mater 2006;B135:171–9.
[7] Rao VVB, Rao SRM. Adsorption studies on treatment of textile dyeing industrial effluent by flyash. Chem Eng J 2006;116:77–84.
[8] Wang CC, Juang LC, Hsu TC, Lee CK, Lee CF, Huang FC. Adsorption of basic dyes onto montmorillonite. J Colloid Interface Sci 2004;273:80–6.
[9] Monvisade P, Siriphannon P. Chitosan intercalated montmorillonite: preparation, characterization, and cationic dye adsorption. Appl Clay Sci 2009;42:427–31.
[10] Teng MY, Lin SH. Removal of methyl orange dye from water onto raw and acid-activated montmorillonite in fixed beds. Desalination 2006;201:71–81.
[11] Wang L, Wang A. Adsorption properties of Congo Red from aqueous solution onto surfactant-modified montmorillonite. J Hazard Mater 2008;160:173–80.
[12] Liu P, Zhang L. Adsorption of dyes from aqueous solutions or suspensions with clay nano-adsorbents. Sep Purif Technol 2007;58:32–9.
[13] Shen D, Fan J, Zhou W, Gao B, Yue Q, Kang Q. Adsorption kinetics and isotherm of anionic dyes onto organo-bentonite from single and multisolute systems. J Hazard Mater 2009;172:99–107.
[14] Zohra B, Aicha K, Fatima S, Nourredine B, Zoubir D. Adsorption of Direct Red 2 on bentonite modified by cetyltrimethylammonium bromide. Chem Eng J 2008;136:295–305.
[15] Yang Y, Han S, Fan Q, Ugbolue SC. Nanoclay and modified nanoclay as sorbents for anionic, cationic and nonionic dyes. Textile Res J 2005;75(8):622–7.
[16] Juang LC, Wang CC, Lee CK, Hsu TC. Dyes adsorption onto organoclay and MCM-41. J Environ Eng Manage 2007;17(1):29–38.
[17] Thir SS, Rauf N. Removal of a cationic dye from aqueous solutions by adsorption onto bentonite clay. Chemosphere 2006;63:1842–8.
[18] Bouberka Z, Kacha S, Kameche M, Elmaleh S, Derriche D. Sorption study of an acid dye from an aqueous solutions using modified clays. J Hazard Mater 2005;B119:117–24.
[19] Özcan A, Ömeroğlu Ç, Erdoğan Y, Özcan AS. Modification of bentonite with a cationic surfactant: an adsorption study of textile dye Reactive Blue 19. J Hazard Mater 2007;140:173–9.
[20] Yapar S. Physicochemical study of microwave-synthesized organoclays. Colloids Surf A Physicochem Eng Asp 2009;345:75–81.
[21] Yılmaz N, Yapar S. Adsorption properties of tetradecyl- and hexadecyl trimethylammonium bentonites. Appl Clay Sci 2004;27:223–8.
[22] Alkan M, Çelikçapa S, Demirbaş Ö, Doğan M. Removal of reactive blue 221 and acid blue 62 anionic dyes from aqueous solutions by sepiolite. Dyes Pigments 2005;65:251–9.
[23] Tabak A, Eren E, Afsin B, Caglar B. Determination of adsorptive properties of a Turkish sepiolite for removal of Reactive Blue 15 anionic dye from aqueous solutions. J Hazard Mater 2009;161:1087–94.
[24] Morais LC, Freitas OM, Gonçalves EP, Vasconcelos LT, Gonzalez Beça CG. Reactive dyes removal from wastewaters by adsorption on eucalyptus bark: variables that define the process. Water Res 1999;33(4):979–89.
[25] Pelegrini R, Zamora PP, De Andrede AR, Reyes J, Duran N. Electrochemically assisted photocatalytic degradation of reactive dyes. Appl Catal B Environ 1999;22:83–90.
[26] Dutta S, Parsons SA, Bhattacharjee C, Bandhyopadhyay S, Data S. Development of an artificial neural network model for adsorption and photocatalysis of reactive dye on TiO_2 surface. Exp Syst Appl 2010;37:8634–8.
[27] Daneshvar N, Khataee AR, Djafarzadeh N. The use of artificial neural networks (ANN) for modeling of decolorization of textile dye solution containing C.I. Basic Yellow 28 by electrocoagulation process. J Hazard Mater 2006;B137:1788–95.
[28] Khataee AR. Photocatalytic removal of C.I. Basic Red 46 on immobilized TiO_2 nanoparticles: artificial neural network modeling. Environ. Technol. 2009;30:1155–68.
[29] Salari D, Niaei A, Khataee A, Zarei M. Electrochemical treatment of dye solution containing C.I. Basic Yellow 2 by the peroxi-coagulation method and modeling of experimental results by artificial neural networks. J Electroanal Chem 2009;629:117–25.
[30] Khataee AR, Zarei M, Pourthassan M. Bioremediation of Malachite Green from contaminated water by three microalgae neural network modeling. Clean 2010;38(1):96–103.
[31] Balci B, Keskinkan O, Avcı M. Use of BDST and an ANN model for prediction of dye adsorption efficiency of Eucalyptus camaldulensis barks in fixed-bed system. Exp Syst Appl 2011;38:949–56.
[32] Available from: http://www.accessscience.com/popup.aspx?figID=434400FG0010&id=434400&name=figure [February 2011].
[33] Inthorn D, Singhtho S, Thiravetyan P, Khan E. Decolorization of basic, direct and reactive dyes by pre-treated narrow-leaved cattail (*Typha angustifolia* Linn.). Bioresource Technol 2004;94:299–306.

[34] Wang LK, Langley DF. Determining cationic surfactant concentration. Ind Eng Chem Prod Res Dev 1975;14(3):210–3.
[35] Hameed BH, Ahmad AA, Aziz N. Isotherms, kinetics and thermodynamics of acid dye adsorption on activated palm ash. Chem Eng J 2007;133:195–203.
[36] Hamdaoui O, Naffrechoux E. Modeling of adsorption isotherms of phenol and chlorophenols onto granular activated carbon. J Hazard Mater 2007;147:401–11.
[37] Azizian S. Kinetic models of sorption: a theoretical analysis. J Colloid Interface Sci 2004;276:47–52.
[38] Khataee AR, Dehghan G, Ebadi A, Zarei M, Pourhassan M. Biological treatment of a dye solution by Macroalgae *Chara sp.*: effect of operational parameters, intermediates identification and artificial neural network modeling. Bioresource Technol 2010;101:2252–8.